Noise-induced phase space transport in two-dimensional Hamiltonian systems

Ilya V. Pogorelov*
Department of Physics, University of Florida, Gainesville, Florida 32611

Henry E. Kandrup†
Department of Astronomy, Department of Physics, and Institute for Fundamental Theory, University of Florida, Gainesville, Florida 32611

(Received 11 February 1999)

First passage time experiments were used to explore the effects of low amplitude noise as a source of accelerated phase space diffusion in two-dimensional Hamiltonian systems, and these effects were then compared with the effects of periodic driving. The objective was to quantify and understand the manner in which ''sticky'' chaotic orbits that, in the absence of perturbations, are confined near regular islands for very long times, can become ''unstuck'' much more quickly when subjected to even very weak perturbations. For both noise and periodic driving, the typical escape time scales logarithmically with the amplitude of the perturbation. For white noise, the details seem unimportant: Additive and multiplicative noise typically have very similar effects, and the presence or absence of a friction related to the noise by a fluctuation-dissipation theorem is also largely irrelevant. Allowing for colored noise *can* significantly decrease the efficacy of the perturbation, but only when the autocorrelation time, which vanishes for white noise, becomes so large that there is little power at frequencies comparable to the natural frequencies of the unperturbed orbit. Similarly, periodic driving is relatively inefficient when the driving frequency is not comparable to these natural frequencies. This suggests that noise-induced extrinsic diffusion, like modulational diffusion associated with periodic driving, is a resonance phenomenon. The logarithmic dependence of the escape time on amplitude reflects the fact that the time required for perturbed and unperturbed orbits to diverge a given distance scales logarithmically in the amplitude of the perturbation. [S1063-651X(99)03508-4]

PACS number(s): 05.45.−a, 05.40.Ca, 05.60.Cd

I. MOTIVATION

It is well known that a complex phase space containing large measures of both regular and chaotic orbits is often partitioned by such partial obstructions as cantori [1] or Arnold webs [2] which, although not serving as absolute barriers, can significantly impede the motion of a chaotic orbit through a connected phase space region. Indeed, the fact that, in two-dimensional Hamiltonian systems, chaotic orbits can be ''stuck'' near regular islands for very long times was discovered empirically [3] long before the existence of cantori was proven [4].

It has also been long known that low amplitude stochastic perturbations can accelerate Hamiltonian phase space transport by enabling orbits to traverse these partial barriers. This was, e.g., explored by Lieberman and Lichtenberg [5], who investigated how motion described by the simplified Ulam version of the Fermi acceleration map [6] is impacted by random perturbations, allowing for the modified equations [7]

$$u_{n+1} = |u_n + \psi_n - \tfrac{1}{2}|,$$
$$\psi_{n+1} = \psi_n + \frac{M}{u_{n+1}} + \Delta\psi, \quad \mod 1, \tag{1.1}$$

where the ''noise'' $\Delta\psi$ corresponds to a random phase shift uniformly sampling an interval $[-\varphi, +\varphi]$.

That stochastic perturbations can have such effects on Hamiltonian systems is important in understanding the limitations of simple models of real systems. In the absence of all ''perturbations'' and any other irregularities, the chaotic phase space associated with some idealized two- or three-dimensional Hamiltonian system may be partitioned into regions which are effectively distinct over relatively short time scales. However, even very weak perturbations of the idealized model, so small as to seem irrelevant on dimensional grounds, can blur these barriers and permit a single orbit to move from one region to another on surprisingly short time scales.

One practical setting where this may be important is in understanding how, in the context of the core-halo model [8] of mismatched charged particle beams, the focusing of an accelerator beam can be corrupted by imperfections in the magnetic fields. To the extent that such irregularities can be modeled as noise, there is the concern that noise-induced diffusion can result in particles in the beam becoming sufficiently defocused as to hit the walls of the container, which is a disaster. Work in this area is currently focused on obtaining realistic estimates of the noise amplitude and the form of the power spectrum [9].

Another setting is in galactic astronomy. Recent observations indicating (i) that many/most galaxies are genuinely triaxial, i.e., neither spherical nor axisymmetric, and (ii) that they contain a pronounced central mass concentration suggest strongly that the self-consistently determined bulk gravi-

*Electronic address: ilya@phys.ufl.edu
†Electronic address: kandrup@astro.ufl.edu

tational potential associated with a galaxy contains significant measures of both regular and chaotic orbits [10]. It was originally expected that, in such complex potentials, regular orbits would provide the skeleton to support the triaxial structure, and that chaotic orbits would serve to fill in the remaining flesh of the self-consistent equilibrium [11]. However, it appears that, in many cases, much of the expected role of regular orbits must be played by ''sticky'' chaotic orbit segments since, as a result of resonance overlap, the measure of regular orbits in certain critical regions is very small, albeit nonzero [12]. The obvious question is, can low amplitude perturbations reflecting internal substructures like gas clouds and individual stars or the effects of an external environment destabilize a near-equilibrium on a time scale short compared with the age of the Universe? Preliminary work would suggest that they can [13].

In both these settings, one knows that weak perturbations will eventually trigger significant changes in energy on some fiducial relaxation time t_R, which implies that they could have a significant effect. This, however, is not the critical issue here. Rather, the question is whether low amplitude perturbations can have significant effects already on a time scale short compared with the time scale on which the value of the energy, or any other isolating integral, changes significantly.

In understanding the potential effects of such low amplitude ''noise,'' there are at least three important questions which need to be addressed.

(i) *How does the effect depend on the amplitude of the noise?* Is there a threshold amplitude below which the noise is essentially irrelevant, or do the effects turn on more gradually? Does the efficacy of the perturbation scale as a simple power of the amplitude or does one see something more subtle?

(ii) *To what extent do the details of the noise matter?* For some problems, such as energy barrier penetration, additive (i.e., state-independent) and multiplicative (i.e., state-dependent) noises can yield very different results [14]. However, the physics here is not the same since one is not dealing with a barrier which, in the absence of perturbations, is absolute. Rather, one is dealing with an *entropy barrier* [15]. It would seem that the problem of diffusion through cantori or along an Arnold web is more similar to problems involving chaotic scattering [16] or escapes of unbound orbits from a complex Hamiltonian system [17] where, in the absence of perturbations, the requisite escape channels exist and it is only a matter of how fast any given orbit can find one.

(iii) *Why does noise lead to accelerated phase space transport?* Granted that the physics is different from diffusion in energy, what is the correct physics? One possibility is that introducing noise simply fuzzes out the details of a purely Hamiltonian evolution that are ensured by Liouville's theorem, thus enabling orbits to breach gaps which would otherwise be impenetrable. However, something very different might be responsible for what is seen.

This paper aims to address these questions for two-dimensional Hamiltonian systems by performing *first passage time experiments.* What this entails is identifying chaotic orbits which, in the absence of any perturbations, remain ''stuck'' near regular islands for very long times, and determining how the introduction of weak noise reduces the escape time. The experiments that were performed and interpreted involved both additive and multiplicative noise. They also allowed for both white noise, which is δ-correlated in time and has a flat power spectrum, and colored noise, which has a finite autocorrelation time, so that the power spectrum effectively cuts off for large frequencies. Finally, the experiments allowed for both external noise, presumed to exist in and of itself, and internal noise, which is accompanied by a friction that is related to the noise by a fluctuation-dissipation theorem [18]. To gain additional insights, the results of these noisy experiments were also compared with experiments in which the unperturbed initial conditions were evolved in the presence of low amplitude periodic driving, so that the breaching of cantori could be triggered by modulational diffusion [7].

Section II describes the experiments that were performed, and the following three sections report the results. Section III summarizes the effects of low amplitude periodic driving, indicating the relative importance of the amplitude and frequency of the perturbation. Section IV describes the effects of different sorts of white noises, and Sec. V generalizes the preceding section to the case of colored noise. Section VI concludes by summarizing the evidence that, like periodic driving, noise-induced extrinsic diffusion through cantori is a resonance phenomemon which requires substantial power at frequencies comparable to the natural frequencies of the unperturbed orbit, and which has an efficacy that scales logarithmically in the amplitude of the perturbation.

II. A DESCRIPTION OF THE COMPUTATIONS

The experiments described here were performed for orbits evolved in two representative two-dimensional potentials, namely the so-called dihedral potential [19] for one particular set of parameter values, for which the Hamiltonian takes the form

$$H=\frac{1}{2}(p_x^2+p_y^2)-(x^2+y^2)+\frac{1}{4}(x^2+y^2)^2-\frac{1}{4}x^2y^2, \tag{2.1}$$

and the sixth-order truncation of the Toda lattice potential [20], for which

$$H=\frac{1}{2}(p_x^2+p_y^2)+\frac{1}{2}(x^2+y^2)+x^2y-\frac{1}{3}y^3+\frac{1}{2}x^4+x^2y^2+\frac{1}{2}y^4+x^4y+\frac{2}{3}x^2y^3-\frac{1}{3}y^5+\frac{1}{5}x^6+x^4y^2+\frac{1}{3}x^2y^4+\frac{11}{45}y^6. \tag{2.2}$$

Extensive explorations of orbits in these Hamiltonians would suggest that, in many respects, these potentials are generic in the set of nonintegrable potentials admitting global stochasticity. This is consistent with the fact that the experiments performed for this paper yielded similar results for both potentials. However, these potentials *are* special in the sense that they admit discrete symmetries: the dihedral potential is invariant under a rotation by $\pi/4$; the truncated Toda potential is invariant under a rotation by $2\pi/3$. It should be noted

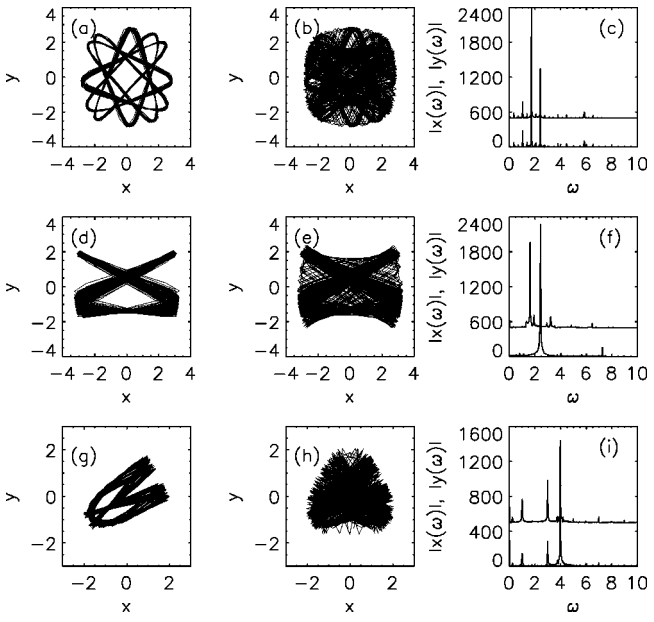

FIG. 1. (a) A chaotic initial condition with $E=10$ evolved in the dihedral potential for a time $t=512$. (b) The same orbit integrated for $t=1024$. (c) The power spectra $|x(\omega)|$ and $|y(\omega)|$ for the orbit in (a). (d) A chaotic initial condition with $E=20$ evolved in the dihedral potential for a time $t=512$. (e) The same orbit integrated for $t=1024$. (f) $|x(\omega)|$ and $|y(\omega)|$ for the orbit in (d). (g) A chaotic initial condition with $E=20$ evolved in the truncated Toda potential for a time $t=300$. (h) The same orbit integrated for $t=600$. (i) $|x(\omega)|$ and $|y(\omega)|$ for the orbit in (g).

for future reference that, for relatively low energies, $E<40$ or so, a characteristic orbital time scale in each potential corresponds to a time $t\sim 1-3$, so that most of the power in typical orbits is in frequencies $\omega\sim 1-5$.

In both potentials it is easy to find ''sticky'' [3] chaotic orbits which, visually, are very nearly indistinguishable from regular orbits for comparatively long times (although they have short time Lyapunov exponents sufficiently large that they must be chaotic). Three examples are exhibited in the left hand panels of Fig. 1, namely two orbits in the dihedral potential, with energies $E=10$ and $E=20$, and an orbit in the truncated Toda potential with $E=20$. The orbit in Fig. 1(a) resembles closely what a galactic astronomer would term a regular loop orbit; the orbit in Fig. 1(d) resembles a regular fish. The orbit in Fig. 1(g) is less familiar, but would again seem nearly regular. The important point, then, is that if the orbit is integrated for a somewhat longer interval, its behavior exhibits an abrupt qualitative change. This is illustrated in the center panels of Fig. 1, which exhibit the same initial conditions, each integrated for an interval twice as long. The first two orbits are no longer centrophobic, and the third has so changed as to manifest explicitly the discrete $2\pi/3$ rotation symmetry of the truncated Toda potential. In each case, the orbit is far more chaotic, as is readily confirmed by the computation of a Lyapunov exponent.

The transition from nearly regular, ''sticky'' behavior to something more manifestly chaotic occurs once the orbit has diffused through one or more cantori that surround a regular phase space island [1,4]. The orbit starts out chaotic and remains chaotic throughout, but its basic properties exhibit significant qualitative changes after the orbit has escaped through the cantori to become ''unconfined.'' The precise objective of the work described here is to determine how the time required for chaotic orbits to change from sticky to unconfined is altered when the orbit is perturbed by low amplitude perturbations.

Determining the precise location of the outermost cantorus is possible, albeit exceedingly tedious [21]. Fortunately, however, this is not essential in order to estimate with reasonable accuracy when a ''sticky'' orbit has become ''unstuck.'' Once the orbit has breached the outermost confining cantorus, it will typically move quickly to probe large portions of the accessible configuration space regions, which were inaccessible before this escape. Moreover, escape is accompanied by an abrupt increase in the value of the largest short time Lyapunov exponent [22], which reflects the fact that ''sticky'' chaotic orbit segments confined near regular islands tend to be less unstable than unconfined chaotic segments far from any regular island [23].

As a practical matter, the *first escape time* for a sticky chaotic orbit was identified by (i) using simple polynomial formulas to delineate approximately the configuration space region to which the orbit is originally confined, and then (ii) determining the first time that, with or without perturbations, the orbit leaves this special region. To check that the escape criterion was reasonable, two tests were performed: It was verified that, with or without perturbations, small changes in the precise definition have only minimal effects on the computed first escape time, and that, for the case of unperturbed orbits, the time of escape corresponds to a time when the largest short time Lyapunov exponent exhibits an abrupt increase.

This prescription allowed one to identify with reasonable accuracy transitions from sticky chaotic to unconfined chaotic behavior, but *not* from chaotic to regular. The constant energy surface contains KAM tori, which serve as absolute boundaries between regular and chaotic behavior, so that an unperturbed orbit that starts as chaotic can never become regular. If, however, the orbit is perturbed, the energy is no longer conserved, and it becomes possible in some cases for an orbit which began as chaotic to evolve to a state in which, if the noise were terminated, would be regular.

The experiments described in this paper involved generating ensembles of perturbed orbits and then extracting statistical properties from these ensembles. In this setting, two different diagnostics proved especially useful.

(i) *The time T(0.01) required for 1% of the orbits in the ensemble to escape.* As described in the following sections, escapes do not begin immediately. Rather, there is typically a relatively extended initial period, the duration of which depends on the form of the perturbation, during which no escapes are observed. Perhaps the most obvious number to record would be the time when the first orbit in the ensemble escapes. However, it was found that, in a non-negligible fraction of the experiments that were performed — perhaps 5–10 % — one orbit often escapes long before any of the others. For this reason, it seemed more reasonable to track a diagnostic that is less sensitive to comparatively rare exceptions.

(ii) *The initial escape rate* Λ. In many, albeit not all, cases it was found that, once the escape process ''turns on'' at (say) time t_0, orbits escape in a fashion which, at least

initially, is consistent with a Poisson process, with $N(t)$, the fraction of the orbits which have not escaped, decreasing exponentially:

$$N(t) = N_0 \exp[-\Lambda(t-t_0)]. \tag{2.3}$$

The experiments with periodic driving involved solving an evolution equation of the form

$$\frac{d^2\mathbf{r}}{dt^2} = -\nabla V(\mathbf{r}) + A\sin(\omega t+\varphi)\hat{\mathbf{r}}. \tag{2.4}$$

The driving was thus characterized by three parameters, namely the frequency ω, the amplitude A, and the phase φ. Usually, but not always, the phase φ was set equal to zero. Ensembles of periodically driven orbits were generated by (i) specifying a frequency interval $[\omega, \omega+\Delta]$, (ii) sampling this interval uniformly to select a collection of (usually) 1000 driving frequencies, and then (iii) integrating the same initial condition with the same amplitude A for each of these frequencies. When looking at relatively low frequencies, $0 < \omega < 100$, the frequency range was taken to be $\Delta = 1.0$. For higher frequencies, $100 < \omega < 1000$, the range $\Delta = 10.0$.

The experiments involving intrinsic noise entailed solving Langevin equations of the form

$$\frac{d^2\mathbf{r}}{dt^2} = -\nabla V(\mathbf{r}) - \eta\mathbf{v} + \mathbf{F}, \tag{2.5}$$

with $\eta = \eta(\mathbf{v})$ and $\mathbf{F}$ homogeneous Gaussian noise characterized by its first two moments:

$$\langle F_a(t)\rangle = 0$$

and

$$\langle F_a(t_1)F_b(t_2)\rangle = \delta_{ab}K(\mathbf{v}, t_1-t_2) \quad (a,b=x,y). \tag{2.6}$$

$K(\mathbf{v},\tau)$ is the autocorrelation function. For the case of δ-correlated white noise,

$$K(\mathbf{v},\tau) = 2\Theta\,\eta(\mathbf{v})\,\delta_D(\tau), \tag{2.7}$$

where Θ denotes a characteristic temperature, the friction and noise being related by a fluctuation-dissipation theorem. Experiments involving extrinsic noise proceeded identically, except that the friction was turned off, so that

$$\frac{d^2\mathbf{r}}{dt^2} = -\nabla V(\mathbf{r}) + \mathbf{F}. \tag{2.8}$$

White noise simulations were performed using an algorithm developed by Griner *et al.* [24] (see also [25]). Colored noise simulations were performed using a more complex algorithm described in Sec. V. The experiments with δ-correlated white noise allowed both for additive noise, where η is a constant, and multiplicative noise, where η is a nontrivial function of $\mathbf{v}$. The experiments with colored noise involved two different choices for the form of $K(\tau)$, in each case allowing for a parameter α which characterized the temporal width of the autocorrelation function. In every case, ensembles of orbits with the same initial conditions were generated by freezing the form and amplitude of the noise and performing multiple realizations of the same random process using different pseudorandom seeds.

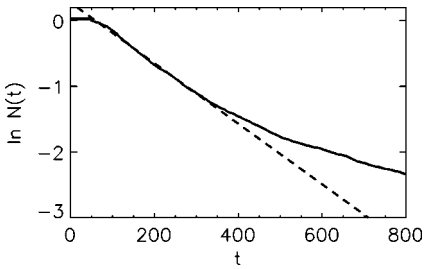

FIG. 2. $N(t)$, the fraction of the orbits from a 4001 orbit ensemble not yet having escaped at time t, computed for the initial condition exhibited in Fig. 1(a), allowing for a perturbation of amplitude $A = 10^{-2.5}$ with variable frequencies $2.0 \leqslant \omega \leqslant 3.0$.

III. PERIODIC DRIVING AND MODULATIONAL DIFFUSION

Experiments involving multiple integrations of the same initial condition reveal that escape is (at least) a two-stage process: In general, there is an initial interval, often quite extended, during which no escapes occur. Only after this interval is there an abrupt onset of escapes which, at least for relatively early times, can be well modeled as a Poisson process, where $N(t)$, the fraction of the orbits that have not yet escaped, decreases exponentially. An example of this behavior is illustrated in Fig. 2, which was generated for the initial condition exhibited in Fig. 1(a), allowing for a frequency interval $2.0 \leqslant \omega \leqslant 3.0$ and an amplitude $A = 10^{-2.5}$. The straight line exhibits a linear fit to the interval $T(0.01) \leqslant t \leqslant 300$.

As asserted already, at a time only somewhat larger than $T(0.01)$, $N(t)$ appears to decrease exponentially. However, for $t > 400$ or so it is clear from Fig. 2 that $N(t)$ decreases more slowly. One plausible interpretation of this later subexponential decay is that some of the initially sticky chaotic orbits have become trapped even closer to the regular island, so that escape becomes much more difficult if not impossible. This interpretation was tested by turning off the periodic driving at a late time $t = 1024$ and computing both the orbit and an approximation to the largest short time Lyapunov exponent for the interval $1024 < t < 3072$. The resulting output indicated that, in the absence of any driving, many of these orbits were now regular.

For fixed frequency interval and phase, both $T(0.01)$, a measure of the time before escapes begin, and Λ, the initial escape rate once escapes have begun, typically scale logarithmically in A, the amplitude of the driving. Six examples of this behavior are provided in Fig. 3, these corresponding to the three initial conditions exhibited in Fig. 1 for two different frequency intervals, namely $0.0 \leqslant \omega \leqslant 1.0$ and $2.0 \leqslant \omega \leqslant 3.0$. In each case, the size of the error bar has been set equal to the difference between $T(0.01)$ and the time at which the first orbit escapes. In most cases, this difference is small, but in some cases it becomes appreciable. The fact that the curve is not exactly linear, and that it levels out for certain ranges of amplitude, is not an obvious finite number effect. Doubling the number of frequencies that were

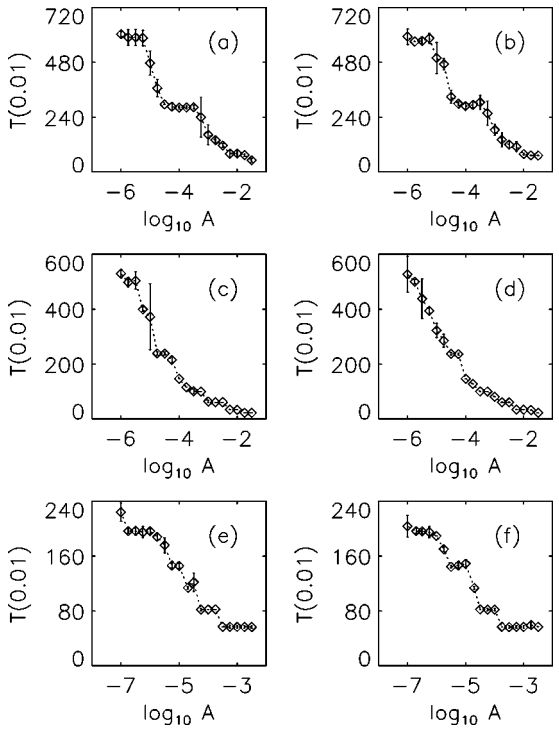

FIG. 3. (a) $T(0.01)$, the first escape time for 1% of an ensemble of 1000 integrations of the initial condition of Fig. 1(a), driven with frequencies $0 \leqslant \omega \leqslant 1$, plotted as a function of the logarithm of the amplitude A of the perturbation. (b) The same for an ensemble with $3 \leqslant \omega \leqslant 4$. (c) $T(0.01)$, the first escape time for 1% of an ensemble of 1000 integrations of the initial condition of Fig. 1(d), driven with frequencies $0 \leqslant \omega \leqslant 1$, plotted as a function of the logarithm of the amplitude A of the perturbation. (d) The same for an ensemble with $3 \leqslant \omega \leqslant 4$. (e) $T(0.01)$, the first escape time for 1% of an ensemble of 1000 integrations of the initial condition of Fig. 1(g), driven with frequencies $0 \leqslant \omega \leqslant 1$, plotted as a function of the logarithm of the amplitude A of the perturbation. (f) The same for an ensemble with $3 \leqslant \omega \leqslant 4$.

sampled, and hence the number of orbits, does not significantly impact the overall smoothness of the curve.

Before the onset of escapes, the rms deviation $\delta r_{\rm rms}$ between perturbed and unperturbed orbits typically grows as

$$\delta r_{\rm rms} \propto A \exp(\chi t), \tag{3.1}$$

where A is the driving amplitude and χ is comparable to the positive short time Lyapunov exponent for the unperturbed orbit. The rms deviation $\delta E_{\rm rms}$ also varies linearly with A, but exhibits a much weaker time dependence. That both these quantities scale linearly in A is hardly surprising, since periodic driving is a coherent process. The different time dependences reflect the fact that, although nearby chaotic orbits tend to diverge exponentially in configuration space, with or without small perturbations, energy is conserved absolutely in the absence of perturbations. That $T(0.01)$ scales as $\log_{10} A$ means that escapes begin when $\delta r_{\rm rms}$, rather than $\delta E_{\rm rms}$, assumes a roughly constant value, independent of the amplitude A. The characteristic value when escapes begin is typically $\delta r_{\rm rms} \sim 1-2$, which implies that the perturbed orbits have dispersed to probe most of the region inside the confining cantori.

This leads to a natural interpretation of the escape process: Early on, the perturbed orbits remain relatively close to the unperturbed orbit, so that it is unlikely that they will be able to escape. (The initial conditions were so chosen that, in the absence of perturbations, escape only occurs at a comparatively late time.) Eventually, however, the perturbed orbits will have spread out to sample more or less uniformly some region inside the bounding cantori. Once this has happened, orbits will begin to escape ''at random'' in a fashion that samples a Poisson process. If the holes were very large, one might expect that the escape rate at this stage would be nearly independent of amplitude. Given, however, that orbits still have to ''hunt'' for tiny escape channels, one might expect that Λ also depends logarithmically on the amplitude of the perturbation.

This interpretation is consistent with the expectation that an initially localized ensemble of chaotic orbits will exhibit an exponential in time approach towards a near-invariant distribution that corresponds to a near-uniform population of those accessible phase space regions not obstructed by cantori [26]. It is also qualitatively similar to what appears to happen when considering the escape of energetically unbound orbits from a complicated two-dimensional potential [27].

Periodic driving tends to yield the smallest $T(0.01)$ and largest Λ for driving frequencies ω comparable to the natural frequencies of the unperturbed orbits. For example, a plot of $T(0.01)$ as a function of ω for fixed amplitude A and phase φ typically exhibits the smallest values of $T(0.01)$ for $\omega \sim 1-3$ and an abrupt increase for somewhat larger frequencies. However, low amplitude driving can still have an appreciable effect on the time of escape even when the driving frequency is much larger than the natural frequencies of the unperturbed orbit. For example, $T(0.01)$ can be significantly shorter than the escape time for an unperturbed orbit even for driving frequencies as large as $\omega \sim 1000$.

Three examples of how $T(0.01)$ varies with ω for fixed A and ϕ are exhibited in Fig. 4. The three left panels plot $T(0.01)$ as a function of ω for $0 \leqslant \omega \leqslant 40$. The three right panels plot $T(0.01)$ as a function of $\log_{10} \omega$ for $1 \leqslant \omega \leqslant 1000$. In some cases $T(0.01)$ varies smoothly as a function of ω for $\omega \gg 10$; in other cases, considerably more irregularity is evident. In either case, however, it is apparent that, overall, the efficacy of the driving is set by the logarithm of the driving frequency. $T(0.01)$ tends to increase linearly in $\log_{10} \omega$. Given the plausible hypothesis that this accelerated escape is a resonance phenomenon involving a coupling between the driving frequency and the natural frequencies of the unperturbed orbits, the fact that high frequencies still have an appreciable effect can be interpreted as implying that, even though the unperturbed orbit has little power at high frequencies, periodic driving can couple via higher order harmonics.

When, for fixed A and φ, $T(0.01)$ and Λ are comparatively smooth functions of driving frequency, $T(0.01)$ tends to exhibit only a relatively weak dependence on the phase. Different values of φ tend to yield comparable escape times. If, alternatively, $T(0.01)$ depends sensitively on ω, it is more likely that the escape time also depends sensitively on φ. However, this trend is not uniform. In some cases, varying φ continuously from 0 to 2π changes $T(0.01)$ by no more than

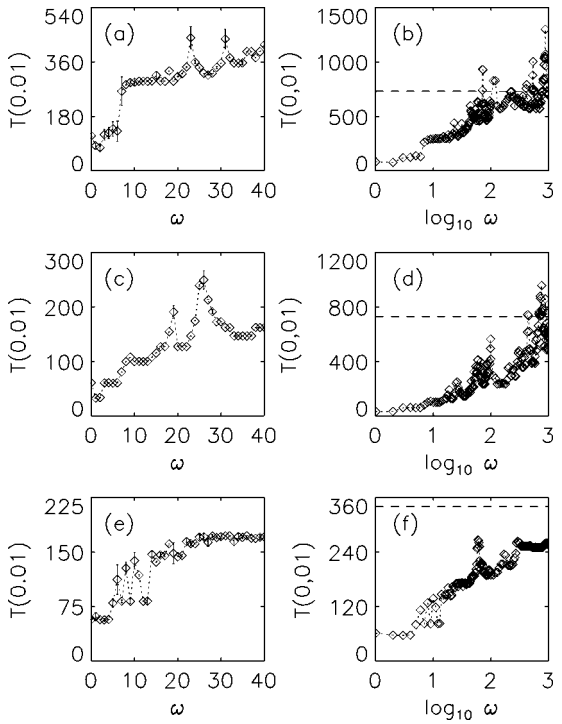

FIG. 4. (a) $T(0.01)$, the first escape time for 1% of an ensemble of 1000 integrations of the initial condition of Fig. 1(a), driven with amplitude $A=10^{-2.5}$, plotted as a function of frequency range $\omega \leqslant \Omega < \omega+1$ for $0<\omega<40$. (b) The same information for $1<\omega<1000$, now plotted as a function of $\log_{10}\omega$. The dashed line represents the escape time for the unperturbed orbit. (c) $T(0.01)$, the first escape time for 1% of an ensemble of 1000 integrations of the initial condition of Fig. 1(c), driven with amplitude $A=10^{-2.5}$, plotted as a function of frequency range $\omega \leqslant \Omega < \omega+1$ for $0<\omega<40$. (d) The same information for $1<\omega<1000$, now plotted as a function of $\log_{10}\omega$. The dashed line represents the escape time for the unperturbed orbit. (e) $T(0.01)$, the first escape time for 1% of an ensemble of 1000 integrations of the initial condition of Fig. 1(e), driven with amplitude $A=10^{-2.5}$, plotted as a function of frequency range $\omega \leqslant \Omega < \omega+1$ for $0<\omega<40$. (f) The same information for $1<\omega<1000$, now plotted as a function of $\log_{10}\omega$. The dashed line represents the escape time for the unperturbed orbit.

10%. In other cases, $T(0.01)$ can vary by a factor of 4, or more. Finally, it should be noted that the importance of noise in accelerating diffusion through cantori can depend sensitively on the details of the orbit. Consider, e.g., two initial conditions in the same potential with the same energy which probe nearby phase space regions and which, in the absence of perturbations, lead to orbits that escape at comparable times. There is no guarantee that ensembles of periodically driven orbits generated from these different initial conditions and evolved with the same amplitudes, phases, and driving frequencies will exhibit similar values of $T(0.01)$ and Λ, even if the unperturbed orbits have power spectra that are almost identical.

IV. WHITE NOISE

For stationary Gaussian white noise with zero mean, everything is characterized by the autocorrelation function $K(t_1-t_2)=\Theta\,\eta(\mathbf{r},\mathbf{v})\,\delta_D(t_1-t_2)$, the form of which is determined in turn by η. Choosing η to be constant yields additive noise. Allowing for a nontrivial dependence on $\mathbf{r}$ or $\mathbf{v}$ yields multiplicative noise. One aim of the work described here was to determine the extent to which the detailed form of the noise matters. This was done by first performing experiments involving additive noise, and then comparing the results with experiments that involved multiplicative noise of two forms, namely, $\eta \propto v^2$ and $\eta \propto v^{-2}$, where v denotes the orbital speed. The importance of friction was tested by comparing experiments that included a friction related to the noise by a fluctuation-dissipation theorem [18] with experiments with no friction at all.

If the friction and noise are to mimic internal degrees of freedom that are ignored in a mean field description, one anticipates on dimensional grounds that the temperature Θ will be comparable to a typical orbital energy. For this reason, most of the experiments that were performed, including those described here, involved freezing the temperature at a value $\Theta \sim E$ and exploring the effects of varying the amplitude of η. The relative normalizations of the multiplicative and additive noises were fixed by setting

$$\eta(\mathbf{v}) = \eta_0 (v/\langle v \rangle)^{\pm 2}, \tag{4.1}$$

where η_0 denotes the constant η appropriate for additive noise and $\langle v \rangle$ denotes the average speed of the unperturbed orbit. Comparing additive and multiplicative noise entailed comparing experiments with the same η_0.

Considering only two forms of multiplicative noise involves probing the tip of an iceberg: other multiplicative noises could in principle have very different effects. However, the two cases examined here do allow one to ask whether the overall effect of the friction and noise can change significantly if one allows the statistics of the noise to vary along an orbit. The particular forms chosen here were motivated by two considerations. (i) If the noise is intended to mimic discreteness effects in a plasma or a galaxy (i.e., electrostatic or gravitational Rutherford scattering), the friction should depend on velocity [28]. (ii) Allowing for a relatively strong dependence on speed, $\eta \propto v^{\pm 2}$, should make even relatively small differences comparatively easy to see.

Overall, the effects of white noise are very similar to the effects of periodic driving. In particular, escape was again observed to be a two-stage process, involving an initial interval during which different realizations of the same initial condition diverge inside the confining cantori, followed by an abrupt onset of escapes which, at least initially, is well approximated as a Poisson process. Moreover, as for the case of periodic driving, $N(t)$ decreases subexponentially at late times, possibly because some of the noisy orbits have become more closely trapped near a regular island.

Figure 5 exhibits plots of $\ln N(t)$ generated for one representative initial condition, corresponding to the orbit in Fig. 1(a). Here the experiments involved additive noise and friction related by a fluctuation-dissipation theorem, with a fixed $\Theta=10$ and $10^{-9} \leqslant \eta_0 \leqslant 10^{-4}$. It is evident that, as η_0 decreases and the friction and noise become weaker, the escape time $T(0.01)$ increases and the escape rate Λ decreases.

More careful examination reveals further that, for fixed Θ, both $T(0.01)$ and Λ scale logarithmically in η_0. This is illustrated in Fig. 6, which exhibits $T(0.01)$ and a best-fit value of Λ for the ensembles used to construct Fig. 5 (along

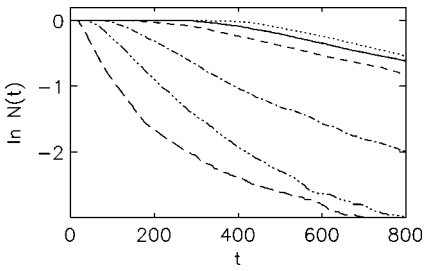

FIG. 5. $N(t)$, the fraction of the orbits from a 2000 orbit ensemble not yet having escaped at time t, computed for the initial condition exhibited in Fig. 1(a), allowing for additive white noise with $\Theta=10$ and variable $\eta=10^{-4}$ (broad dashes), $\eta=10^{-5}$ (triple-dot-dashed), $\eta=10^{-6}$ (dot-dashed), $\eta=10^{-7}$ (narrow dashes), $\eta=10^{-8}$ (solid), and $\eta=10^{-9}$ (dots).

with some ensembles with intermediate values of η). This logarithmic dependence can be understood by analogy with what was observed for periodic driving if one notes that, in the presence of noise, the rms deviation between perturbed and unperturbed orbits typically scales as

$$\delta r_{\rm rms} \propto (\eta\Theta)^{1/2} \exp(\chi t), \tag{4.2}$$

a conclusion that can be motivated theoretically [29] and has been confirmed computationally [13].

It is interesting that this two-stage evolution — an epoch without escapes followed by an epoch with escapes apparently sampling a Poisson process — can also be observed in the absence of noise if one considers a strongly localized ensemble of initial conditions trapped near a regular island and ascertains the time at which each member of the ensemble escapes. For example, an ensemble of orbits sampling a cell of size 0.002 centered about the initial condition used to generate Fig. 6 yielded $T(0.01)=310$ and $\Lambda=0.000\,587$, which should be compared with the values $T(0.01)=131$ and $\Lambda=0.001\,53$ resulting for a single initial condition evolved with $\eta=10^{-9}$.

Perhaps the most significant conclusion about white noise is that, at least for the examples considered here, the details are largely irrelevant. For fixed Θ and η_0, the values of the escape time $T(0.01)$ and the decay rate Λ are both essentially the same for the simulations with additive noise and those with multiplicative noise with $\eta \propto v^{\pm 2}$. The computed values of $T(0.01)$ and Λ are also nearly independent of whether or not one allows for a friction term. The only significant differences between simulations with and without friction arise at late times when the energies of individual

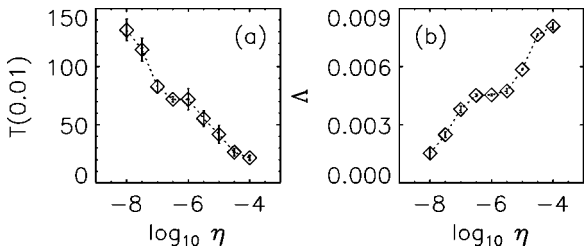

FIG. 6. (a) $T(0.01)$, the first escape time for 1% of an ensemble of 2000 white noise integrations of the initial condition of Fig. 1(a), with $\Theta=10$ and variable η. (b) Λ, the rate at which orbits in this ensemble escape, fitted to the interval $T(0.01)<t<256$.

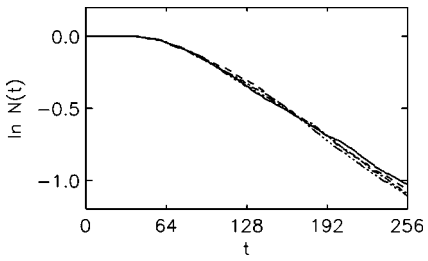

FIG. 7. $N(t)$, the fraction of the orbits from a 2000 orbit ensemble not yet having escaped at time t, computed for the initial condition exhibited in Fig. 1(a) with $\Theta=10$ and $\eta_0=10^{-5}$. The four curves represent additive white noise and constant η (solid), additive white noise with no friction (dashed), multiplicative noise with $\eta \propto v^2$ (dot-dashed), and multiplicative noise with $\eta \propto v^{-2}$ (triple-dot-dashed).

orbits have changed appreciably from their initial values. In this case, allowing for a friction term to counterbalance the noise assures that, overall, the energies of the orbits exhibit smaller changes, so that the ensembles that evolved with noise tend to have somewhat smaller changes in energy.

An example of this insensitivity is provided in Fig. 7, which was generated from orbits with the initial condition of Fig. 1(a), with $\Theta=10$ and $\eta_0=10^{-5}$. The solid, dot-dashed, and triple-dot-dashed curves exhibit $\ln N(t)$ for ensembles evolved in the presence of both friction and noise, incorporating, respectively, additive noise, multiplicative noise with $\eta_0 \propto v^2$, and multiplicative noise with $\eta_0 \propto v^{-2}$. The dashed curve corresponds to an ensemble evolved with additive noise in the absence of friction. The obvious point is that, for a very long time, these curves are nearly indistinguishable.

This insensitivity is again consistent with the hypothesis that noise-induced diffusion through cantori is a resonance phenomenon, and that the only thing that matters is that the noise have significant power at frequencies comparable to the natural frequencies of the unperturbed orbit. If, however, one alters the form of the autocorrelation function so as to suppress power at frequencies comparable to these natural frequencies, one would expect that the effects of the noise should decrease, so that $T(0.01)$ increases and Λ decreases. The extent to which this is true is discussed in Sec. V.

V. COLORED NOISE

The objective of the experiments described here was to explore the effects of random perturbations with autocorrelation times sufficiently long that they cannot be modeled as δ-correlated white noise. Once again it was assumed that the noise is stationary and Gaussian with zero mean and, for simplicity, attention was restricted to noise that is additive. However, it was no longer assumed that $K(\tau)$ is δ-correlated in time.

Attention was focused on two types of colored noise. The first is generated by the Ornstein-Uhlenbeck process (see, e.g., [18]), and is characterized by an autocorrelation function $K(\tau)$ that decays exponentially, i.e.,

$$K(\tau)=\sigma_{\rm col}^2 \exp(-\alpha|\tau|). \tag{5.1}$$

The second involves an exponential decay modulated by a power law:

$$K(\tau)=\sigma_{\rm col}^2\exp(-\alpha|\tau|)\left(1+\alpha|\tau|+\frac{\alpha^2}{3}\tau^2\right). \quad (5.2)$$

The corresponding spectral densities are, respectively,

$$S(\omega)=\frac{\sigma_{\rm col}^2}{\pi}\frac{\alpha}{\omega^2+\alpha^2} \quad (5.3)$$

and

$$S(\omega)=\frac{8\sigma_{\rm col}^2}{3\pi}\frac{\alpha^5}{(\omega^2+\alpha^2)^3}. \quad (5.4)$$

The autocorrelation times are $t_c=1/\alpha$ and $t_c=2/\alpha$. In both cases, white noise corresponds to a singular limit with $\alpha\rightarrow\infty$ and $\sigma_{\rm col}^2\rightarrow\infty$, but $\sigma_{\rm col}^2/\alpha\rightarrow$ const. As for the case of multiplicative noise, these two examples only probe the tip of an iceberg. However, an analysis of their effects *does* provide insight into the question of how a finite autocorrelation time can impact phase space transport in a complex phase space.

Generating white noise numerically is comparatively straightforward, requiring little more than producing a sequence of pseudorandom impulses. Generating colored noise takes more thought. The algorithm exploited here was motivated by the recognition that, in the context of a stochastic differential equation, a white noise random process $X(t)$ can serve as a source to define a colored noise process $Y(t)$. As a concrete example, consider how Gaussian white noise can be used to implement a random process with an autocorrelation function given by Eq. (5.2).

Given one stochastic process, $X(t)$, one can define a second stochastic process, $Y(t)$, implicitly as a solution to the stochastic differential equation

$$\frac{d^3Y(t)}{dt^3}+3\alpha\frac{d^2Y(t)}{dt^2}+3\alpha^2\frac{dY(t)}{dt}+\alpha^3Y(t)=X(t). \quad (5.5)$$

Since the coefficients in Eq. (5.5) are time-independent constants and $X(t)$ is stationary, it is clear that, if this equation be solved as an initial value problem, at sufficiently late times $Y(t)$ can also be considered stationary provided only, as is true, that the dynamical system (5.5) is stable.

By expressing $X(t)$ and $Y(t)$ in terms of their Fourier transforms, it is easy to see that, neglecting the effects of nontrivial boundary conditions (e.g., choosing boundary conditions at $t_0\rightarrow-\infty$), the spectral densities $S_X(\omega)$ and $S_Y(\omega)$ for the two processes satisfy

$$S_Y(\omega)=\frac{S_X(\omega)}{(\omega^2+\alpha^2)^3}. \quad (5.6)$$

Assuming, however, that $X(t)$ corresponds to white noise, $S_X(\omega)\equiv\sigma_X^2$ is a constant, so that the stochastic process with spectral density S_Y necessarily corresponds to colored noise. Indeed, by performing an inverse Fourier transform, it becomes evident that $S_Y(\omega)$ corresponds to the stochastic process (5.2) with

$$\sigma_{\rm col}^2=3\pi\sigma_X^2/(8\alpha^5). \quad (5.7)$$

A colored random process defined by the Langevin equation (2.5) or Eq. (2.8), with an autocorrelation function of the form (5.2), is equivalent mathematically to a collection of white noise processes. Solving Eq. (5.5) for $Y(t)$ yields the colored input required to solve Eq. (2.5) or Eq. (2.8).

The one remaining question involves normalizations. To compare different colored noises with each other or with an appropriately defined white noise limit, one must decide what should be meant by noise with variable autocorrelation time but fixed amplitude. This was done here by considering sequences of random processes with different values of α and, for each α, selecting $\sigma_{\rm col}^2$ such that

$$\int_{-\infty}^{\infty}K_\alpha(\tau)d\tau=\int_{-\infty}^{\infty}K_{\rm white}(\tau)d\tau. \quad (5.8)$$

In other words, fixed amplitude but variable autocorrelation time was assumed to correspond to different colored noises for which the time integral of the autocorrelation function assumes the same value. Noting that

$$\int_{-\infty}^{\infty}K_{\rm white}(\tau)d\tau=2\Theta\eta, \quad (5.9)$$

it follows that, for the stochastic process (5.2),

$$K(\tau)=\frac{3\alpha\eta\Theta}{8}\exp(-\alpha|\tau|)\left(1+\alpha|\tau|+\frac{\alpha^2}{3}\tau^2\right). \quad (5.10)$$

The Ornstein-Uhlenbeck process requires a normalization,

$$K(\tau)=\alpha\eta\Theta\exp(-\alpha|\tau|). \quad (5.11)$$

In the experiments modeling intrinsic noise, the colored noise was augmented by a friction η, and the friction and noise were related by a linear fluctuation-dissipation theorem in terms of a temperature Θ. In the experiments modeling extrinsic noise, the friction vanished and Θ had no independent meaning as a temperature. Aside from α, which fixes the autocorrelation time, all that matters is the quantity $\eta\Theta$, which sets the amplitude of the noise.

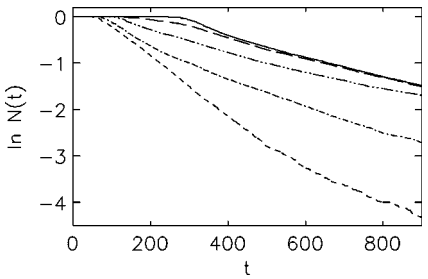

FIG. 8. $N(t)$, the fraction of the orbits from a 4800 orbit ensemble not yet having escaped at time t, computed for the initial condition exhibited in Fig. 1(a), allowing for friction and additive Ornstein-Uhlenbeck noise with $\alpha=0.2$, $\Theta=10$, and variable $\eta=10^{-4}$ (dashed), $\eta=10^{-5}$ (dot-dashed), $\eta=10^{-6}$ (double-dot-dashed), $\eta=10^{-7}$ (broad-dashed), and $\eta=10^{-8}$ (solid).

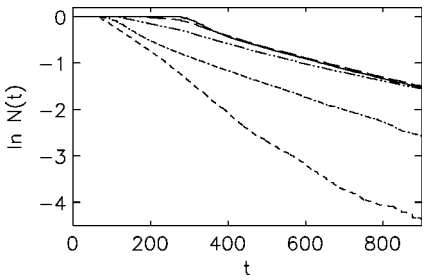

FIG. 9. $N(t)$, the fraction of the orbits from a 4800 orbit ensemble not yet having escaped at time t, computed for the initial condition exhibited in Fig. 1(a), allowing for friction and colored noise given by Eq. (5.2) with $\alpha=0.2$, $\Theta=10$, and variable $\eta=10^{-4}$ (dashed), $\eta=10^{-5}$ (dot-dashed), $\eta=10^{-6}$ (double-dot-dashed), $\eta=10^{-7}$ (broad-dashed), and $\eta=10^{-8}$ (solid).

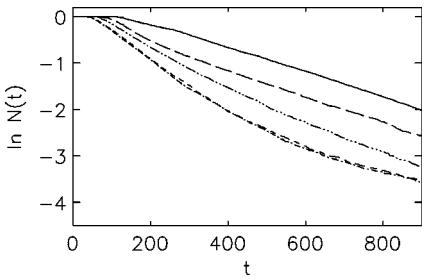

FIG. 11. $N(t)$, the fraction of the orbits from a 4800 orbit ensemble not yet having escaped at time t, computed for the initial condition exhibited in Fig. 1(a), allowing for friction and colored noise given by Eq. (5.2) with $\Theta=10$, $\eta=10^{-5}$, and either white noise (dashes) or variable $\alpha=20$ (dot-dashed), $\alpha=2.0$ (triple-dot-dashed), $\alpha=0.2$ (broad dashes), and $\alpha=0.02$ (solid).

As for white noise, the evolution of an ensemble of noisy colored orbits is a two-stage process. After an initial epoch without escapes, during which different members of the ensemble diverge exponentially, escapes turn on abruptly, with the first percent of the orbits escaping within an interval $T(0.01)$ much shorter than the time before the first escape. Interestingly, though, the second phase is often more complex than what is observed for white noise. Instead of evolving in a fashion that is well fit pointwise by an exponential decrease, the number remaining, $N(t)$, often exhibits ''plateaus'' and ''jumps'' with (almost) no, and especially large, decreases. (A detailed examination of the data reveals that such irregularities can also arise for white noise and periodic driving, but are usually much less conspicuous in that case.)

Figures 8–11 exhibit $\ln N(t)$ generated for an initial condition where such irregularities are comparatively small. Figures 8 and 9 exhibit data generated for different 4800 orbit ensembles generated, respectively, for the stochastic processes (5.1) and (5.2), for the same initial condition as Fig. 5, evolved with $\Theta=10.0$, $\alpha=0.2$, and variable η. Figures 10 and 11 exhibit analogous plots for the same initial condition with $\eta=10^{-5}$ and variable α. Figure 12 exhibits data for a second initial condition in the same potential with the same energy for which the early-time irregularities are especially conspicuous.

These irregularities imply that a pure exponential fit is often not justified. Moreover, even when such a fit *is* justified, one finds that, for fixed α, significantly different values of η can yield very similar slopes [30]. In this sense, it is not accurate to state unambiguously that the escape rate scales logarithmically with amplitude. However, what does remain true is that, overall, escapes tend to happen more slowly in the presence of lower amplitude perturbations, and that any systematic amplitude dependence is very weak, certainly much weaker than a simple power law $\propto \eta^{-p}$ with p of order unity. Moreover, even though the observed escape rates exhibit considerable irregularities, the 1% escape time $T(0.01)$ does not. As for the case of white noise and periodic driving, $T(0.01)$ scales logarithmically in amplitude. Several examples are exhibited in Figs. 13(a) and 13(c), which plot $T(0.01)$ as a function of $\log_{10}\eta$ for two different initial conditions. In each case, the diamonds represent an Ornstein-Uhlenbeck process and the triangles the stochastic process (5.2). In panel (a) $\alpha=2.0$; in panel (c) $\alpha=0.2$.

As for white noise, one also finds that, seemingly independent of α, the presence or absence of friction is largely irrelevant. This is, e.g., evident from Table I, which, for two values of α, namely $\alpha=\infty$ (white noise) and $\alpha=0.02$ (autocorrelation time $\tau=50$), exhibits $T(0.01)$ as a function of $\log_{10}\eta$ both in the presence and the absence of friction.

Another obvious conclusion is that the efficacy of colored noise is a decreasing function of α, the quantity that sets the autocorrelation time t_c. When α is very large, so that t_c is extremely short, color has virtually no effect. However, as α decreases and t_c increases, $T(0.01)$ increases. In particular, for $\alpha \ll 1$, which corresponds to an autocorrelation time that is long compared to a characteristic orbital time scale, $T(0.01)$ is typically much longer than what is found in the white noise limit. This behavior is evident from Figs. 13(b) and 13(d), which exhibit $T(0.01)$ as a function of $\log_{10}\alpha$ for fixed $\eta=10^{-5}$. As for Figs. 13(a) and 13(c), the diamonds

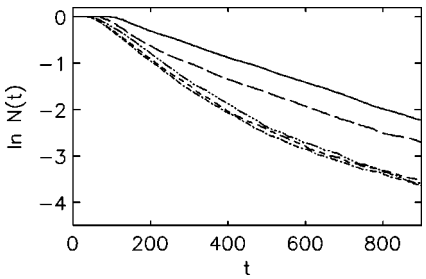

FIG. 10. $N(t)$, the fraction of the orbits from a 4800 orbit ensemble not yet having escaped at time t, computed for the initial condition exhibited in Fig. 1(a), allowing for friction and Ornstein-Uhlenbeck noise, with $\Theta=10$, $\eta=10^{-5}$, and either white noise (dot-dashed) or variable $\alpha=20$ (dashed), $\alpha=2.0$ (triple-dot-dashed), $\alpha=0.2$ (broad dashes), and $\alpha=0.02$ (solid).

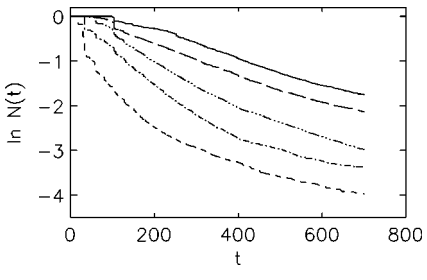

FIG. 12. The same as Fig. 8 for a different initial condition.

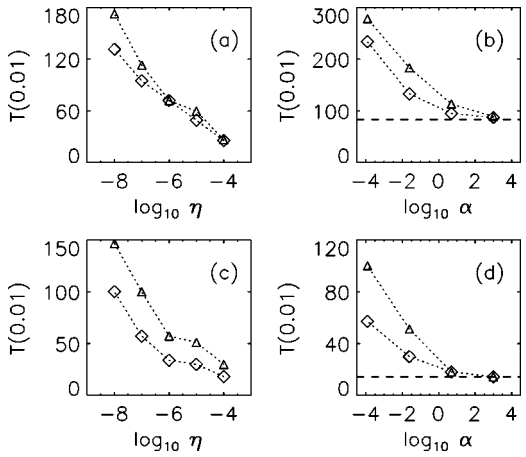

FIG. 13. (a) $T(0.01)$, the first escape time for 1% of an ensemble of 4800 integrations, computed for the initial condition used to generate Fig. 1(a), plotted as a function of $\log_{10}\eta$ for fixed $\alpha=2.0$ for the stochastic processes defined by Eq. (5.1) (diamonds) and Eq. (5.2) (triangles), allowing for both friction and noise. (b) $T(0.01)$ for the same initial condition, plotted as a function of $\log_{10}\alpha$ for fixed $\eta=10^{-5}$, for the stochastic processes (5.1) (diamonds) and (5.2) (triangles), again allowing for both friction and noise. The dashed line represents the asymptotic value for white noise ($\alpha\to\infty$). (c) The same as (a), albeit for a different initial condition and with $\alpha=0.2$. (d) The same as (b), albeit for the initial condition in (c) and with $\eta=10^{-7}$ as (a) and (b) for another initial condition.

and triangles represent, respectively, the stochastic processes (5.1) and (5.2). The horizontal dashed line represents the white noise value towards which the data converge for $\alpha\to\infty$. The obvious inference from this, and other, plots is that the dependence of $T(0.01)$ on α or t_c is again roughly logarithmic. This is reminiscent of the fact that, as discussed in Sec. III, the efficacy of periodic driving tends to scale logarithmically in the driving frequency.

Determining the overall efficacy of colored noise as a source of accelerated phase space transport thus involves an interplay between amplitude and autocorrelation time, each of which, in the ''interesting'' regions of parameter space, contributes logarithmically to $T(0.01)$ and (modulo the aforementioned caveats) Λ.

VI. DISCUSSION

Just as for diffusion triggered by low amplitude periodic driving, the overall efficacy of noise-induced diffusion of ''sticky'' chaotic orbits scales logarithmically in the amplitude of the perturbation. For both white and colored noise, the 1% escape time $T(0.01)$ scales logarithmically in the amplitude of the perturbation and, at least for white noise, so does the initial escape rate. The details of the perturbation seem largely unimportant: The presence or absence of a friction term appears immaterial, and allowing for (at least some forms of) multiplicative noise also has comparatively minimal effects. For the case of white noise, the only thing that seems to matter is the amplitude.

TABLE I. The 1% escape time $T(0.01)$ for orbits in an ensemble evolved in the dihedral potential (2.1) with the initial condition used to generate Fig. 1(a), setting $\Theta=10.0$ and allowing for variable η. The colored noise was generated by the stochastic process (5.2).

$\log_{10}\eta$	$\alpha=\infty$ with friction	$\alpha=\infty$ no friction	$\alpha=0.02$ with friction	$\alpha=0.02$ no friction
−4	21.621	21.672	71.930	71.811
−5	41.740	41.660	113.024	112.980
−6	71.863	71.816	172.396	172.393
−7	82.744	82.724	277.684	277.682
−8	131.368	131.616	277.704	277.709

This logarithmic dependence on amplitude implies that what regulates the overall efficacy of the noise in inducing phase space transport is how fast perturbed noisy orbits diverge from the original unperturbed orbit. Escapes entail a two-stage process, namely (i) an early interval during which noisy orbits diverge from the unperturbed orbit without breaching cantori and (ii) a later interval during which, in many cases, orbits escape seemingly at random in a fashion that samples a Poisson process. That $T(0.01)$ scales logarithmically in amplitude reflects the fact that escapes typically begin once $\delta r_{\rm rms}$, the rms separation between perturbed and unperturbed orbits, approaches a critical value comparable to the size of the region in which the ''sticky'' orbits are originally stuck. That the escape rate tends in many cases to exhibit at least a rough logarithmic dependence reflects the fact that, even after the noisy orbits have spread out to sample a near-invariant population inside the confining cantori, random kicks can facilitate phase space transport by helping the orbits to ''find'' holes in the cantori.

That escapes begin when $\delta r_{\rm rms}$, rather than $\delta E_{\rm rms}$, approaches a critical value has an important implication for how one ought to envision the escape process. Naively, it is not completely obvious whether friction and noise facilitate phase space transport by ''jiggling'' individual orbits or, since they change the orbital energy, by ''jiggling'' the effective phase space hypersurface in which the orbits move. The fact that $\delta r_{\rm rms}$ sets the scale on which things happen demonstrates that, in point of fact, the former interpretation is more natural.

The apparent fact that extrinsic diffusion can be viewed as a random process is seemingly consistent with what has been observed in the context of simple maps representing kicked oscillators [31]. Experiments tracking the evolution of an ensemble of particles originally trapped within a stochastic web and recording the number in the web as a function of time reveal an initial epoch during which all the particles are in the web, the duration of which is a decreasing function of the noise amplitude, followed by an epoch during which the number decreases, which terminates in the approach towards an asymptotic state corresponding, presumably, to an equilibrium between transits into and out of the web.

Allowing for colored noise can significantly reduce the rate of phase space transport, but only when the autocorrelation time t_c becomes comparable to, or larger than, a characteristic crossing time. If the noise is such that the spectral density $S(\omega)$ has only minimal power at frequencies comparable to the natural frequencies of the unperturbed orbit, its efficacy in inducing accelerated phase space transport will be reduced significantly. For α sufficiently large and t_c sufficiently small, the two colored noises that were explored yield essentially the same results as did white noise; and similarly,

for α sufficiently small and t_c sufficiently long, the effects of the noise must become essentially negligible, so that one recovers the behavior observed for an unperturbed orbit. For intermediate values, however, the escape statistics *do* depend on the value of α. Moreover, this dependence is reminiscent of the effects of periodic driving in at least one important respect: For the case of periodic driving, quantities like $T(0.01)$ exhibit a roughly logarithmic dependence on the driving frequency ω. For the case of colored noise, $T(0.01)$ exhibits a roughly logarithmic dependence on α.

This would suggest that, like modulational diffusion triggered by periodic driving, noise-induced phase space diffusion is intrinsically a resonance phenomenon. If the Fourier transform of the noise has appreciable power in the frequency range where the unperturbed orbit has appreciable power, noise-induced diffusion will be comparatively efficient. If, however, the noise has little power at such frequencies, it will serve as a much less efficient agent for phase space transport, although the effects need not be completely negligible.

To the extent that, as suggested by the numerical experiments described here, the details are relatively unimportant, the effects of noise as a source of phase space transport are determined by two physical quantities, namely (i) the amplitude and (ii) the autocorrelation time. Increasing the amplitude makes noise more important; increasing the autocorrelation time makes noise less important.

As a concrete example, consider stars orbiting in an elliptical galaxy comparable in size to the Milky Way but located in the central part of a cluster like Coma, where the typical distance between galaxies is only five to ten times larger than the diameter of a typical galaxy. Here there are two obvious sources of noise which one might consider, namely (i) ''discreteness effects'' reflecting the fact that the galaxy is made of individual stars rather than a dustlike continuum and (ii) the near-random influences of the surrounding environment. Discreteness effects result in gravitational Rutherford scattering, which can be modeled reasonably [28] by friction and δ-correlated white noise related by a fluctuation-dissipation theorem where, in natural units, $\eta \sim 10^{-7}-10^{-9}$. To the extent that the near-random influences of the surrounding environment can be attributed primarily to a small number of neighboring galaxies, it is also easy to estimate their amplitude and typical autocorrelation time. Given that the nearest-neighboring galaxy is typically separated by a distance $\sim 5-10$ times the diameter of the galaxy in question, and that the relative velocities of different galaxies in a cluster are usually comparable to the typical velocities of stars within an individual galaxy, one expects that the autocorrelation time t_* is of order 5–10 characteristic orbital times $t_{\rm cr}$. Presuming, however, that the perturbing influences of nearby galaxies reflect tidal effects, their overall strength should scale as D^{-3}, where D is the distance from the galaxy in question, so that a typical amplitude $\eta \sim 10^{-3}-10^{-2}$.

In this setting, discreteness effects give rise to comparatively weak noise with a very short autocorrelation time. Environmental effects give rise to a considerably stronger noise with a much longer autocorrelation time. The longer autocorrelation time tends to suppress the effects of environmental noise, but, even so, it would seem likely that, as a source of accelerated phase space transport, environmental noise will be significantly more important than discreteness noise.

ACKNOWLEDGMENTS

The authors acknowledge useful discussions with Salman Habib and Katja Lindenberg. Partial financial support was provided by the Institute for Geophysics and Planetary Physics at Los Alamos National Laboratory. The simulations involving colored noise were performed using computational facilities provided by Los Alamos National Laboratory.

[1] S. Aubry and G. Andre, in *Solitons and Condensed Matter Physics*, edited by A. Bishop and T. Schneider (Springer, Berlin, 1978), p. 264; I. Percival, in *Nonlinear Dynamics and the Beam-Beam Interaction*, edited by M. Month and J. C. Herrara, AIP Conf. Proc. No. 57 (AIP, New York, 1979), p. 302.

[2] V. I. Arnold, Russ. Math. Surveys **18**, 85 (1964).

[3] G. Contopoulos, Astron. J. **76**, 147 (1971); see also R. S. Shirts and W. P. Reinhart, J. Chem. Phys. **77**, 5204 (1982).

[4] J. N. Mather, Topology **21**, 45 (1982).

[5] M. A. Lieberman and A. J. Lichtenberg, Phys. Rev. A **5**, 1852 (1972).

[6] E. Fermi, Phys. Rev. **75**, 1169 (1949).

[7] See, e.g., A. J. Lichtenberg and M. A. Lieberman, *Regular and Chaotic Dynamics* (Springer, Berlin, 1992).

[8] S. Habib and R. Ryne, Phys. Rev. Lett. **74**, 70 (1995).

[9] S. Habib, R. Ryne, and J. Qiang (unpublished); see also S. Habib, H. E. Kandrup, and M. E. Mahon, Phys. Rev. E **53**, 5473 (1996).

[10] J. Kormendy and R. Bender, Astrophys. J. Lett. **464**, 119 (1996); D. Merritt, Science **241**, 337 (1996).

[11] See, e.g., J. Binney, Comments. Astrophys. **8**, 27 (1978).

[12] See, e.g., E. Athanassoula, O. Bienyamé, L. Martinet, and D. Pfenniger, Astron. Astrophys. **127**, 349 (1983); H. Wozniak, in *Ergodic Concepts in Stellar Dynamics*, edited by V. G. Gurzadyan and D. Pfenniger (Springer, Berlin, 1994), p. 264; D. Merritt and T. Fridman, Astrophys. J. **46**, 136 (1996).

[13] S. Habib, H. E. Kandrup, and M. E. Mahon, Astrophys. J. **480**, 155 (1997).

[14] See, e.g., K. Lindenberg and V. Seshadri, Physica A **109**, 481 (1981); F. J. Alexander and S. Habib, Phys. Rev. Lett. **71**, 955 (1993).

[15] J. Machta and R. Zwanzig, Phys. Rev. Lett. **50**, 1959 (1983).

[16] See, e.g., S. Bleher, C. Grebogi, and E. Ott, Physica D **46**, 87 (1990); Y.-T. Lau, J. M. Finn, and E. Ott, Phys. Rev. Lett. **66**, 978 (1991), and references cited therein.

[17] G. Contopoulos, H. E. Kandrup, and D. E. Kaufmann, Physica D **64**, 310 (1993).

[18] See, e.g., N. G. van Kampen, *Stochastic Processes in Physics and Chemistry* (North Holland, Amsterdam, 1981).

[19] D. Armbruster, J. Guckenheimer, and S. Kim, Phys. Lett. A **140**, 416 (1989).

[20] M. Toda, J. Phys. Soc. Jpn. **22**, 431 (1967).

[21] G. Contopoulos (private communication); J. D. Meiss (private communication). In any event, determining with great precision the exact boundary of the sticky region for unperturbed orbits is not well motivated physically: Once the orbit has been perturbed, the value of its energy will have changed, which implies that the boundary is no longer the same.

[22] P. Grassberger, R. Badii, and A. Poloti, J. Stat. Phys. **51**, 135 (1988).

[23] M. E. Mahon, R. A. Abernathy, B. O. Bradley, and H. E. Kandrup, Mon. Not. R. Astr. Soc. **275**, 443 (1995).

[24] A. Griner, W. Strittmatter, and J. Honerkamp, J. Stat. Phys. **51**, 95 (1988).

[25] J. Honerkamp, *Stochastic Dynamical Systems* (VCH Publishers, New York, 1994).

[26] H. E. Kandrup and M. E. Mahon, Phys. Rev. E **49**, 3735 (1994).

[27] H. E. Kandrup, C. Siopis, G. Contopoulos, and R. Dvorak, Chaos (to be published).

[28] S. Chandrasekhar, *Principles of Stellar Structure* (University of Chicago Press, Chicago, 1943).

[29] H. E. Kandrup and D. E. Willmes, Astron. Astrophys. **283**, 59 (1994).

[30] This anomalous behavior tends to arise most often for very small values of η, which suggests that, for sufficiently low amplitude, noise is not all that helpful in allowing an ensemble which has already dispersed to find holes in the confining cantori.

[31] A. J. Lichtenberg and B. P. Wood, Phys. Rev. Lett. **62**, 2213 (1989). See, in particular, Fig. 3.